arXiv:1611.06029v1 [cond-mat.mes-hall] 18 Nov 2016

Multiple gaps in the tight-binding band of a pentagonal lattice

Susobhan Paul*

Department of Physics, Scottish Church College,

Urquhart Square, Kolkata 700006, India

Asim Kumar Ghosh†

Department of Physics, Jadavpur University,

188 Raja Subodh Chandra Mallik Road, Kolkata 700032, India

Abstract

Multiple gaps in the tight-binding band of a pentagonal lattice are found. Unlike the Cairo pentagonal lattice this lattice is made of irregular pentagons with arms of different lengths. The tight-binding Hamiltonian is exactly solved to obtain analytic expressions of dispersion relations and eigenvectors. Four different band-gaps are identified along with two distinct indirect band-gaps at the Harrison point. Multiple band-gaps in this model may give rise to exotic electronic properties.

*Electronic address: suso.phy.paul@gmail.com

†Electronic address: asimkumar96@yahoo.com

I. INTRODUCTION

Tight-binding (TB) analysis on the two-dimensional lattices draws much attentions nowadays for their predictions of exotic electronic properties before the availability of results based on the experimental investigations. Although the regular polygons like triangles, squares and hexagons fill up a plane surface without overlap and leaving any voids, it is impossible to do so by regular pentagons due to its five-fold symmetry. Thus to fill up a plane surface one has to use irregular pentagons. Those irregular pentagons can be derived from the regular one either by changing the angles between the arms keeping its length fixed or by changing both the length of the arms as well as the angles between them. The Cairo pentagonal lattice is made of irregular pentagons with different angles between the arms by keeping their lengths fixed. The recent theoretical study on Cairo pentagonal lattice indicates the presence of a large band-gap. The magnitude of this gap is 3.25 eV which is predicted by density functional theory (DFT). This system is known as penta-graphene (p-graphene) which is essentially a Cairo pentagonal monolayer of carbon atoms[1]. DFT analysis on other Cairo pentagonal monolayers of boron nitride and silver azide similarly indicates the signature of a single band-gap[2]. The TB analysis on p-graphene supports the existence of the same single band-gap whose estimated value is very close to the previous prediction[3]. The nature of optical absorption around this band-gap is studied. The presence of band-gap is also important for the engineering of electronic devices.

In this article we are going to introduce a TB model on another pentagonal lattice that is composed of different types of irregular pentagons (Fig. 1 (a)). For this model multiple band-gaps are observed in the TB analysis rather than a single one. The lattice can be derived from the honeycomb lattice in the following way. The parent (honeycomb) lattice is elongated vertically in such a manner that vertical bonds get doubled in its original length. Additional lattice points are introduced in the middle of each vertical bonds. After joining these additional points this particular structure of pentagonal lattice is obtained. In the resulting lattice, any horizontal layer is made of identical pentagons by placing them side by side without overlapping and leaving any voids. The adjacent layers those are just vertically above or down of this one are made of inverted pentagons. The lattice is non-Bravais. One can visualize this lattice as composed of six interpenetrating rectangular Bravais lattices, those are identical to each other. In Fig. 1 (b), these sublattices are identified by B_1, B_2, B_3,

C_1, C_2 and C_3. Those sublattices can be divided on the basis of their coordination numbers into two types. Coordination number of both B_1 and C_1 is four while it is three for the others. The rectangular unit cell of this lattice is shown in Fig. 1 (c). It contains six lattice points. This lattice has the translational invariance of length $\sqrt{3}\,a$ along the x-direction and that of length $(4+\sqrt{3})\,a$ along the y-direction, where a is the length of shorter arms of the pentagon. It also has rotational invariance of the angle 180°. The first Brillouin zone is shown in Fig. 1 (d).

Very few theoretical results are available for this lattice. The bond-percolation threshold is determined and the stability of collinear Néel-type classical ground state for antiferromagnetic (AFM) Heisenberg system on this lattice is studied. In addition, ground state entropy and energy are estimated for the Ising and AFM Heisenberg models, respectively[5, 6]. On the other hand, based on the Cairo pentagonal lattice structure, geometric frustration of AFM compound, $Bi_2Fe_4O_9$ has been investigated[7]. Another Cairo pentagonal lattice structure that has been experimentally realized is the AFM organic radical crystal, α-2,6-Cl_2-V [=α-3-(2,6-dichlorophenyl)-1,5-diphenylverdazyl][8]. Moreover, it has been proposed that a stable carbon allotrope called p-graphene could be materialized very soon which is entirely composed of Cairo-typed carbon pentagons[1]. The same argument may hold true for another new carbon allotrope based on the pentagonal lattice addressed here.

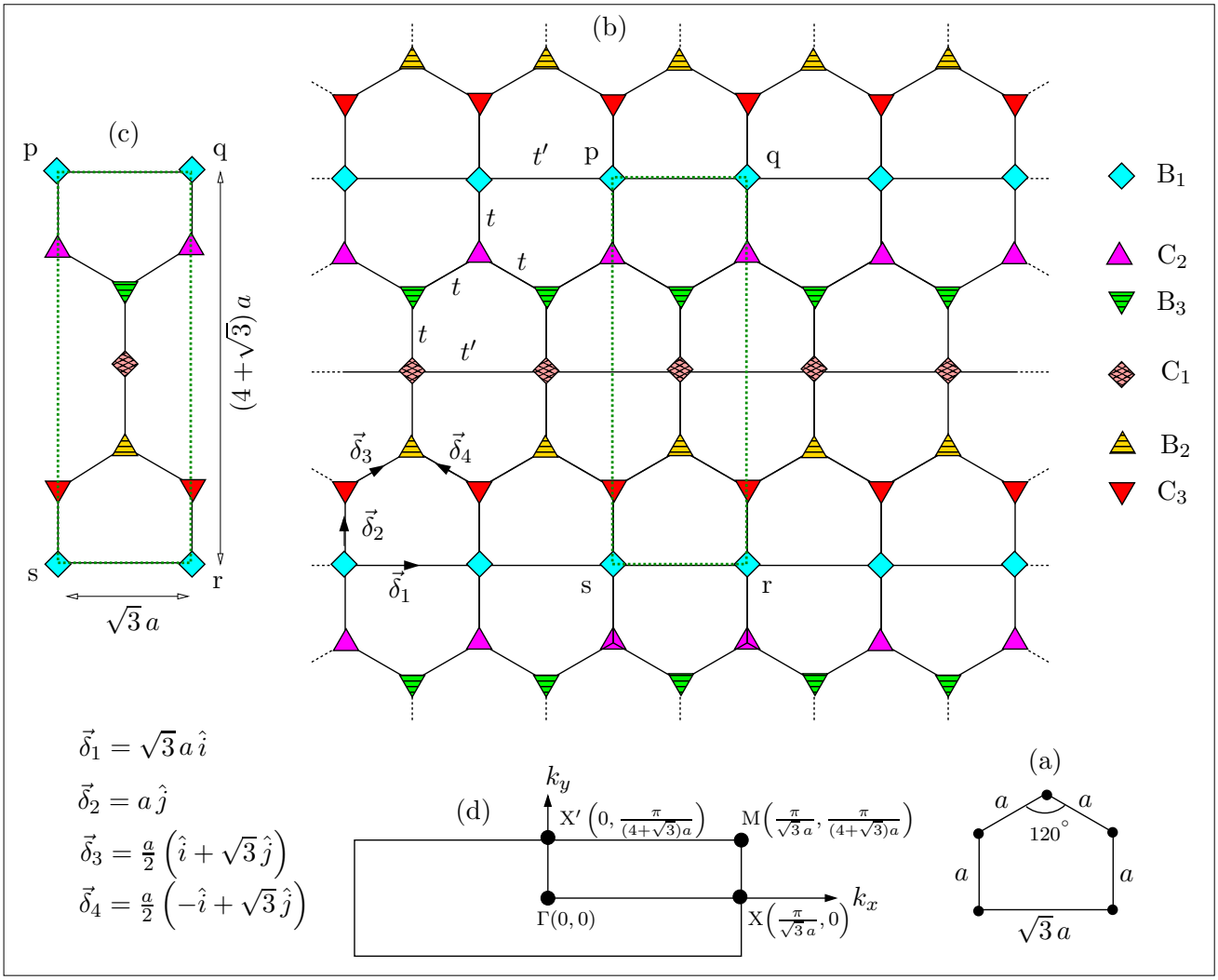

FIG. 1: (Color online) (a) Irregular pentagon, (b) pentagonal lattice, (c) unit cell and (d) first Brillouin zone.

II. THE HAMILTONIAN

Considering only the nearest-neighbor (NN) hoppings, the model is described by the tight-binding Hamiltonian,

$$
\begin{aligned}
H &= \sum_i \left[H_{b_1} + H_{c_2} + H_{b_3} + H_{c_1} + H_{b_2} + H_{c_3}\right], \qquad (1)\\
H_{b_1} &= -t\, b^\dagger_{1,\vec{R}_i}\, c_{3,\vec{R}_i+\vec{\delta}_2} - t'\, b^\dagger_{1,\vec{R}_i}\, b_{1,\vec{R}_i+\vec{\delta}_1} - t\, b^\dagger_{1,\vec{R}_i}\, c_{2,\vec{R}_i-\vec{\delta}_2},\\
H_{c_2} &= -t\, c^\dagger_{2,\vec{R}_i+3\,\vec{\delta}_2+\vec{\delta}_3+\vec{\delta}_4}\, b_{1,\vec{R}_i+4\,\vec{\delta}_2+\vec{\delta}_3+\vec{\delta}_4} - t\, c^\dagger_{2,\vec{R}_i+3\,\vec{\delta}_2+\vec{\delta}_3+\vec{\delta}_4}\, b_{3,\vec{R}_i+3\,\vec{\delta}_2+\vec{\delta}_3}\\
&\quad -t\, c^\dagger_{2,\vec{R}_i+3\,\vec{\delta}_2+\vec{\delta}_3+\vec{\delta}_4}\, b_{3,\vec{R}_i+3\,\vec{\delta}_2+\vec{\delta}_4},\\
H_{b_3} &= -t\, b^\dagger_{3,\vec{R}_i+3\,\vec{\delta}_2+\vec{\delta}_3}\, c_{1,\vec{R}_i+2\,\vec{\delta}_2+\vec{\delta}_3} - t\, b^\dagger_{3,\vec{R}_i+3\,\vec{\delta}_2+\vec{\delta}_3}\, c_{2,\vec{R}_i+3\,\vec{\delta}_2+2\,\vec{\delta}_3}\\
&\quad -t\, b^\dagger_{3,\vec{R}_i+3\,\vec{\delta}_2+\vec{\delta}_3}\, c_{2,\vec{R}_i+3\,\vec{\delta}_2+\vec{\delta}_3+\vec{\delta}_4},\\
H_{c_1} &= -t\, c^\dagger_{1,\vec{R}_i+2\,\vec{\delta}_2+\vec{\delta}_3}\, b_{2,\vec{R}_i+\vec{\delta}_2+\vec{\delta}_3} - t\, c^\dagger_{1,\vec{R}_i+2\,\vec{\delta}_2+\vec{\delta}_3}\, b_{3,\vec{R}_i+3\,\vec{\delta}_2+\vec{\delta}_3},\\
&\quad -t'\, c^\dagger_{1,\vec{R}_i+2\,\vec{\delta}_2+\vec{\delta}_3}\, c_{1,\vec{R}_i+\vec{\delta}_1+2\,\vec{\delta}_2+\vec{\delta}_3},\\
H_{b_2} &= -t\, b^\dagger_{2,\vec{R}_i+\vec{\delta}_2+\vec{\delta}_3}\, c_{1,\vec{R}_i+2\,\vec{\delta}_2+\vec{\delta}_3} - t\, b^\dagger_{2,\vec{R}_i+\vec{\delta}_2+\vec{\delta}_3}\, c_{3,\vec{R}_i+\vec{\delta}_2} - t\, b^\dagger_{2,\vec{R}_i+\vec{\delta}_2+\vec{\delta}_3}\, c_{3,\vec{R}_i+\vec{\delta}_2+\vec{\delta}_3-\vec{\delta}_4},\\
H_{c_3} &= -t\, c^\dagger_{3,\vec{R}_i+\hat{\delta}_2}\, b_{1,\vec{R}_i} - t\, c^\dagger_{3,\vec{R}_i+\hat{\delta}_2}\, b_{2,\vec{R}_i+\hat{\delta}_2+\hat{\delta}_3} - t\, c^\dagger_{3,\vec{R}_i+\hat{\delta}_2}\, b_{2,\vec{R}_i+\hat{\delta}_2+\hat{\delta}_4}.
\end{aligned}
$$

We have considered four closer points to each of A_1 and B_1 sub-lattice sites as the NN points despite their different bond lengths. For other sites, number of NN points are three and their arrangements are like the honeycomb lattice. $\vec{R}_i$ is the Bravais vector for the i-th unit cell. $b^\dagger_j$ ($c^\dagger_j$) is the creation operator at the j-th site with respective orbital for an atom on the B (C) sublattice. t and t' are the parameters of hopping across the NN sites having the bonds of lengths a and $a' = \sqrt{3}a$, respectively (Fig.1 (a)). $\vec{\delta}_i$s are the vectors pointing different adjacent lattice sites within each unit cell. The orbitals are considered to be the simplest one like the π electron of graphene for the sites B_2, B_3, C_2 and C_3. However, no specific orbital structure are assumed for the B_1 and C_1 lattice sites. Ratio of t' and t is parametrized by the quantity, α, where $0 < \alpha < 1$. Thus $t' = \alpha\, t$. Hopping parameters are generally depend on the bond lengths in the system. By using the hopping parameter-bond length relationship introduced by Harrison, *i. e.*, $t(a') \propto 1/a'^{\,2}$, value of α equals to 1/3[4]. This kind of parametrization has been adopted previously for the AFM exchange interaction strengths while investigating the stability of collinear Néel-type classical ground state of Heisenberg Hamiltonian on this pentagonal lattice. Interestingly, the critical value of α, *i. e.*, α_c above which this is no longer so is also very close to 1/3[6].

Hamiltonian is expressed in $\vec{k}$-space by transforming the b and c operators as

$$b_{n\,\vec{k}} = \frac{1}{\sqrt{N}}\, b_{n,\vec{R}_i}\, e^{i\vec{k}\cdot\vec{R}_i}, \quad c_{n\,\vec{k}} = \frac{1}{\sqrt{N}}\, c_{n,\vec{R}_i}\, e^{i\vec{k}\cdot\vec{R}_i}, \quad n = 1, 2, 3,$$

where N is the number of unit cells. By introducing the six component vector,

$$\Psi^\dagger_{\vec{k}} = \left(b^\dagger_{1\,\vec{k}}\;\; b^\dagger_{2\,\vec{k}}\;\; b^\dagger_{3\,\vec{k}}\;\; c^\dagger_{1\,\vec{k}}\;\; c^\dagger_{2\,\vec{k}}\;\; c^\dagger_{3\,\vec{k}}\right),$$

H can be written as

$$H = -t \sum_{\vec{k}} \Psi^\dagger_{\vec{k}}\, H_{\vec{k}}\, \Psi_{\vec{k}}, \tag{2}$$

where the 6×6 Hamiltonian in the momentum space is decomposed in terms of two 3×3 block Hamiltonians, Ω_1 and Ω_2. Therefore,

$$H_{\vec{k}} \;=\; \begin{pmatrix} \Omega_1 & \Omega_2 \\ \Omega_2 & \Omega_1 \end{pmatrix}, \quad \Omega_1 = \begin{pmatrix} X & 0 & 0 \\ 0 & 0 & 0 \\ 0 & 0 & 0 \end{pmatrix}, \quad \Omega_2 = \begin{pmatrix} 0 & Y & Y \\ Y & 0 & Z \\ Y & Z & 0 \end{pmatrix}, \quad \text{where}$$

$$X \;=\; -t' \cos\left(\sqrt{3}\, k_x a\right), \quad Y = -t \cos\left(k_y a\right), \quad \text{and} \quad Z = -2t \cos\left(\frac{k_x a}{2}\right) \cos\left(\frac{\sqrt{3}\, k_y a}{2}\right).$$

The Hamiltonian, $H_{\vec{k}}$ can be diagonalized by introducing the transfer matrix, T such that,

$$H_{\vec{k}} = \Phi^\dagger_{\vec{k}}\, H^d_{\vec{k}}\, \Phi_{\vec{k}}, \quad \Phi_{\vec{k}} = T \Psi_{\vec{k}},$$

where

$$H^{\rm d}_{\vec{k}} = \begin{pmatrix} E^+ & 0 \\ 0 & E^- \end{pmatrix}, \quad T = \begin{pmatrix} T_1 & T_2 \\ T_3 & T_4 \end{pmatrix}, \quad E^\pm = \begin{pmatrix} E_1^\pm & 0 & 0 \\ 0 & E_2^\pm & 0 \\ 0 & 0 & E_3^\pm \end{pmatrix}, \tag{3}$$

$$T_1 = \begin{pmatrix} 0 & \frac{2Y}{(X-E_2^+)\sqrt{N_+}} & \frac{2Y}{(X-E_3^+)\sqrt{N'_+}} \\ -\frac{1}{2} & -\frac{1}{\sqrt{N_+}} & \frac{1}{\sqrt{N'_+}} \\ \frac{1}{2} & -\frac{1}{\sqrt{N_+}} & \frac{1}{\sqrt{N'_+}} \end{pmatrix}, \quad T_2 = \begin{pmatrix} 0 & \frac{2Y}{(X-E_2^-)\sqrt{N_-}} & \frac{2Y}{(X-E_3^-)\sqrt{N'_-}} \\ \frac{1}{2} & -\frac{1}{\sqrt{N_-}} & \frac{1}{\sqrt{N'_-}} \\ -\frac{1}{2} & -\frac{1}{\sqrt{N_-}} & \frac{1}{\sqrt{N'_-}} \end{pmatrix},$$

$$T_3 = \begin{pmatrix} 0 & \frac{2Y}{(X-E_2^+)\sqrt{N_+}} & \frac{2Y}{(X-E_3^+)\sqrt{N'_+}} \\ -\frac{1}{2} & -\frac{1}{\sqrt{N_+}} & \frac{1}{\sqrt{N'_+}} \\ \frac{1}{2} & -\frac{1}{\sqrt{N_+}} & \frac{1}{\sqrt{N'_+}} \end{pmatrix}, \quad T_4 = \begin{pmatrix} 0 & \frac{2Y}{(X-E_2^-)\sqrt{N_-}} & \frac{2Y}{(X-E_3^-)\sqrt{N'_-}} \\ -\frac{1}{2} & -\frac{1}{\sqrt{N_-}} & \frac{1}{\sqrt{N'_-}} \\ \frac{1}{2} & -\frac{1}{\sqrt{N_-}} & \frac{1}{\sqrt{N'_-}} \end{pmatrix},$$

$$N_{\pm} = 4\left(1 + 2\left(\frac{Y}{X - E_2^{\pm}}\right)^2\right), \quad N'_{\pm} = 4\left(1 + 2\left(\frac{Y}{X - E_3^{\pm}}\right)^2\right).$$

$H_{\vec{k}}^{\rm d}$ is the diagonalized Hamiltonian and $\Phi_{\vec{k}}$ is the eigenvector. The exact expressions of six dispersion relations, $E_n^{\pm},\ n = 1, 2, 3$, are written below.

$$\begin{aligned} E_1^{\pm} &= \mp Z, \\ E_2^{\pm} &= \frac{1}{2}\left(X + Z \pm \sqrt{(X - Z)^2 + 8Y^2}\right), \\ E_3^{\pm} &= \frac{1}{2}\left(X - Z \pm \sqrt{(X + Z)^2 + 8Y^2}\right). \end{aligned}$$

The dispersion relations, $E_n^{\pm},\ n = 1, 2, 3$ for $\alpha = 1$ have been drawn in different colors within the first Brillouin zone and shown in Fig. 2. The density of states (DOS), $g(E)$ is derived by using the formula,

$$g(E) = \frac{1}{(2\pi)^2}\int d\vec{k} \sum_{n=1,2,3;\ \gamma=+,-} \delta(E - E_n^{\gamma}(\vec{k})).$$

III. RESULTS AND DISCUSSION

The band-structures due to the six dispersion relations are shown in Fig. 3. Six dispersion relations, E_1^+, E_2^+, E_3^+, E_1^-, E_2^- and E_3^- with DOS for $\alpha = 0, 1/3, 2/3$ and 1 along the q-path, Γ-X-M-X$'$-Γ are drawn in different colors. E_1^+ and E_1^- are symmetric about the zero-energy. No cross-over among the dispersion relations takes place as long as $\alpha \leq 0.41$. While a single cross-over between E_1^+ and E_2^+ occurs beyond that value of α. Four different band-gaps, say, G_n, $n = 1, 2, 3, 4$, are found at different locations. The value of band-gap G_1 (G_2, G_3, G_4) could be obtained from the the difference between the minimum of E_3^+ (E_1^+, E_2^+, E_3^-) and the maximum of E_1^+ (E_2^+, E_3^-, E_1^-). Positions of minimum for E_3^+ and maximum for E_3^- vary with the variation of α. On the other hand, positions of minima for E_1^+, E_2^+ and maxima for E_1^+, E_2^+, E_1^- do not vary with α. So, the minimum values of E_1^+, E_2^+ and maximum values of E_1^+, E_2^+, E_1^- are E_1^+(M), E_2^+(X$'$) and $E_1^+(\Gamma)$, E_2^+(X), E_1^-(M), respectively. E_3^+ is almost flat in the region, M-X$'$ when α is close to 1, giving rise to large value of DOS. Nature of other dispersion relations are of no significance in this study since they do not give rise to band-gap. For $\alpha = 0$, three gaps, G_2, G_3 and G_4 appear. Among them, G_3 is the direct band-gap and symmetric around the zero-energy. G_2 and G_4 are indirect band-gaps

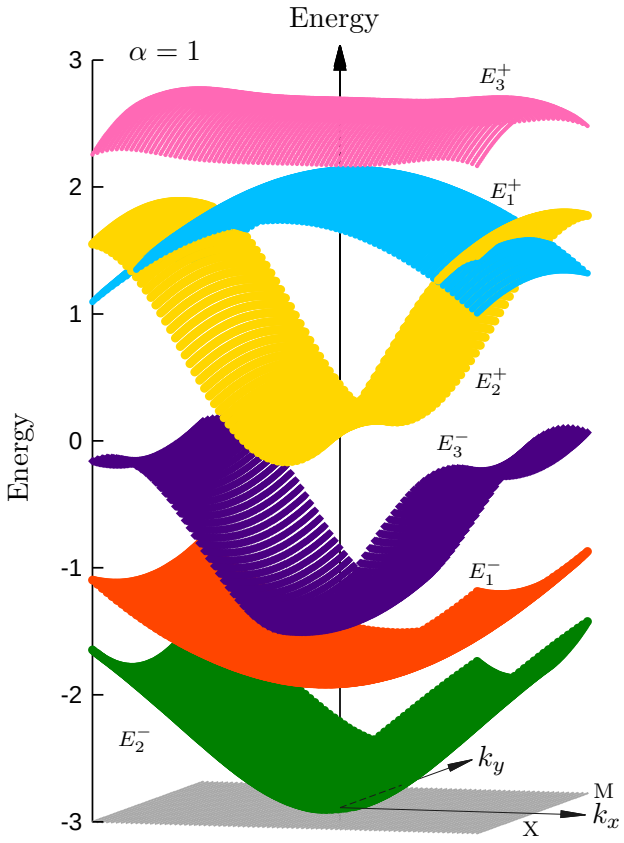

FIG. 2: (Color online) The dispersion relations, E_1^+, E_2^+, E_3^+, E_1^-, E_2^- and E_3^- for $\alpha = 1$ are drawn in different colors within the first Brillouin zone.

and symmetrically arranged about the zero-energy. For $\alpha \neq 0$, only indirect band-gap exists while the symmetries of band-gaps are lost.

Band-gap opens up where DOS vanishes. The band-gap profile of TB bands with respect to α is shown Fig. 4. Widths of G_2 and G_3 have maximum values at $\alpha = 0$, while those for G_4 and G_1 have maximum at $\alpha = 0.13$ and 1.0, respectively. Widths of G_2 and G_3 decrease with the increase of α and exactly vanish at $\alpha = 0.23$ and $\alpha = 1.0$, respectively. However, width of G_4 increases with the increase of α having maximum value at $\alpha = 0.13$. This width afterwards decreases and finally disappears at $\alpha = 0.44$. On the other hand, only one band-gap, G_1 does exist when $\alpha = 1$, and its width steadily decreases with the decrease of α and eventually disappears at $\alpha = 0.41$. By comparing all the four band-gaps it appears that G_3 is the widest gap. The maximum value of this band-gap is observed at X′. Value of this direct band-gap is equal to $E_2^+(\mathrm{X}') - E_3^-(\mathrm{X}') = 1.21t$. At the Harrison point, $\alpha = 1/3$,

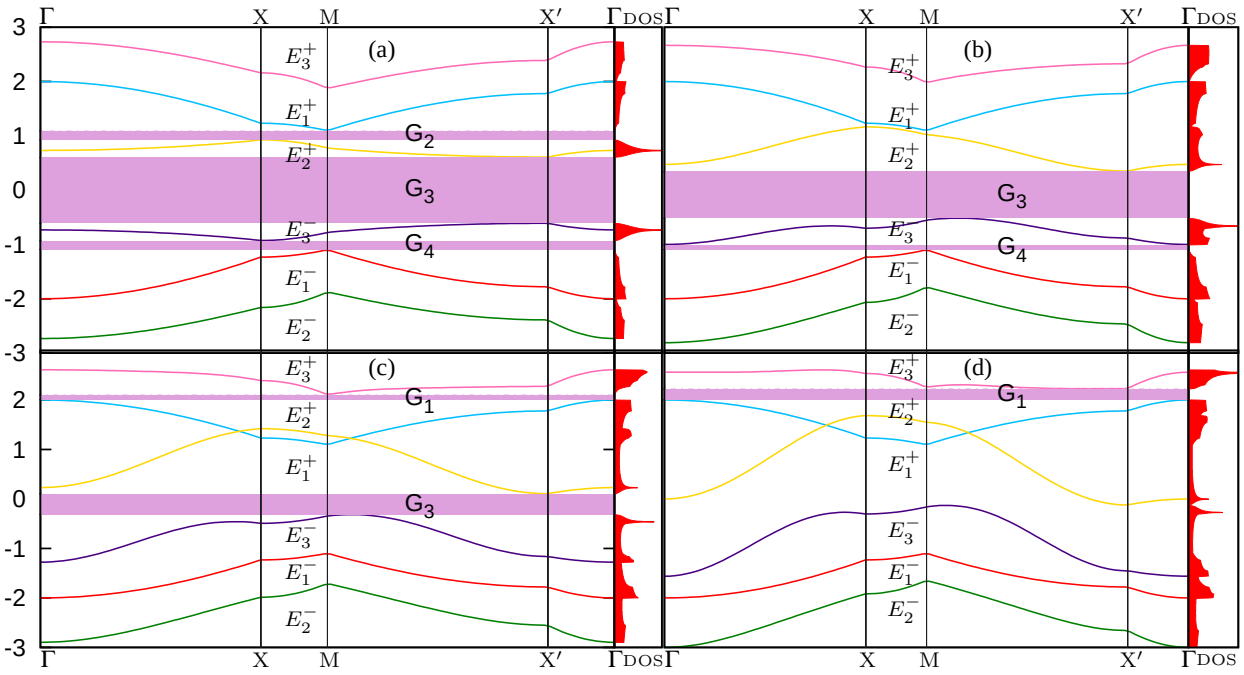

FIG. 3: (Color online) Dispersion relations, E_1^+, E_2^+, E_3^+, E_1^-, E_2^- and E_3^- and DOS for $\alpha = 0$ (a), $\alpha = 1/3$, Harrison point, (b), $\alpha = 2/3$ (c) and $\alpha = 1$ (d) along q-path Γ-X-M-X′-Γ. Four gaps, G_1, G_2, G_3 and G_4 at different locations are shown.

two distinct indirect band-gaps, G_2 and G_4 appear which is indicated by the red-dashed line h in Fig. 4.

In this article, we have clearly predicted the existence of multiple band-gaps in the TB analysis on pentagon lattice in contrast to the previous observation of a single band-gap in the Cairo pentagonal lattice. Like the Cairo pentagonal lattice, no Dirac-cone is found. It would be noted that Dirac-cones are omnipresent in the two-dimensional lattices with the coordination number of three, such as, honeycomb (graphene), 1/2-depleted (T-graphene) and 1/4-depleted square lattices[9]. However, in these pentagonal lattices coordination numbers are either three or four depending on the lattice sites. Recently, innovation of another class of materials, such as p-graphene[1] and heptagraphene[10], resembling the graphene structure are gaining interests in which the basic structure of those lattices are generated

by using the irregular pentagons and heptagons, respectively. This trend is due to the appreciation of exotic electronic properties of graphene. Although, p-graphene is made of only carbon atoms, the unit cell of heptagraphene is composed of ten carbon and four hydrogen atoms. Theoretical studies in the direction of new carbon allotropes predict the possibility of stable p-graphene based on Cairo pentagon, like the stable graphene. Therefore, it is expected that another stable p-graphene based on pentagonal lattice considered here will be materialized very soon. In addition, multiple band-gaps in this pentagonal model might give rise to novel electronic properties.

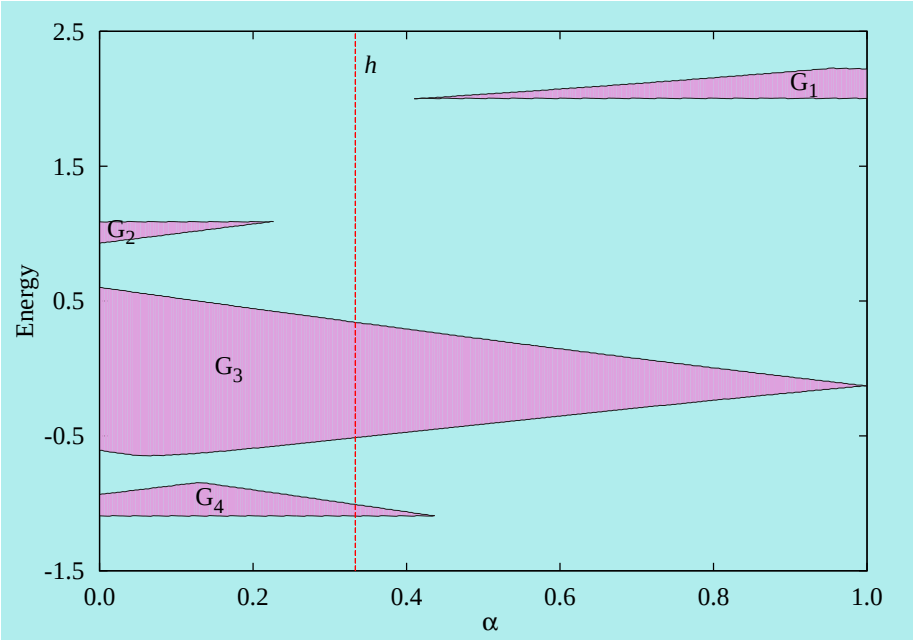

FIG. 4: (Color online) Band-gap profile of the TB band structure with respect to α. Band-gap structure at the Harrison point, h, ($\alpha = 1/3$) is indicated by the vertical dashed (red) line.

Acknowledgments

Authors are grateful to Prof. Indrani Bose for bringing the pentagonal lattice model to their notice. AKG acknowledges a BRNS-sanctioned research project, no. 37(3)/14/16/2015, India.

[1] S. Zhang *et. al.*, Proc. Natl. Acad. Sci. USA **112**, 2372-2377 (2015).

[2] M. Yagmurcukardes *et. al.*, J. App. Phys. **118**, 104303 (2015).

[3] T. Stauber, J. I. Beltran and J. Schliemann, Sci. Rep. **6**, 22672 (2016).

[4] W. A. Harrison, *Elementary Electronic Structure* (World Scientific, 1999), ISBN 981-023895-9.

[5] M. H. Waldor, W. F. Wolf and J. Zittartz, Phys. Lett., **106A**, 261, (1984); Z. Phys. B Condens. Matter **59**, 43 (1985).

[6] U. Bhaumik and I. Bose, Phys. Rev. B **58**, 73 (1998).

[7] E. Ressouche *et. al.*, Phys. Rev. Lett. **103**, 267204 (2009).

[8] H. Yamaguchi *et. al.*, Sci. Rep. **5**, 15327 (2015).

[9] Y. Liu *et. al.*, Phys. Rev. Lett. **108**, 225505 (2012).

[10] A. Lopez-Bezanilla, I. Martin and P. B. Littlewood Sci. Rep. **6**, 33220 (2016).